plants

MDPI

Article

Screening for Cadmium-Tolerant Germplasm and Physiological and Transcriptomic Responses to Cadmium Stress in *Lagerstroemia indica*

Mengjiao Wang [1,2,3], Jinfeng Wang [2,3], Zhiyang Qian [1,2], Gen Meng [1,2,3], Qing He [4], Zhuomei Chen [2,3,*] and Longjie Ni [1,2,3,*]

[1] College of Forestry (College of Life Sciences), Zhejiang A&F University, Hangzhou 311300, China; mengjiaowang325@163.com (M.W.); qianzhiyang2001@163.com (Z.Q.)
[2] Institute of Forest Breeding, Zhejiang Academy of Forestry, Hangzhou 310023, China; wangjinfeng@zjforestry.ac.cn
[3] Zhejiang Key Laboratory of Forest Genetics and Breeding, Hangzhou 210037, China
[4] Hangzhou Yuanjian Landscape Architecture Co., Ltd., Hangzhou 310000, China; zjzmz@126.com
* Correspondence: zhuomeichen@163.com (Z.C.); longjieni@njfu.edu.cn (L.N.)

Abstract

Crape myrtle (*Lagerstroemia indica* L.) is a common ornamental tree species in China, but its physiological responses to cadmium (Cd) stress and variation in Cd tolerance remain unclear. To identify Cd-tolerant materials suitable for cultivation in Cd-contaminated areas, 25 crape myrtle seedling materials were subjected to Cd stress under hydroponic conditions, and seedling growth, photosynthetic pigment contents, antioxidant enzyme activities, osmotic adjustment substances, and membrane lipid peroxidation were analyzed. Cd tolerance was evaluated using principal component analysis combined with a membership function method. Furthermore, rooted cuttings of the Cd-tolerant material YZ21C and the Cd-sensitive material DHZX were used to measure photosynthetic pigments, malondialdehyde (MDA), and organ-specific Cd concentrations, followed by transcriptome sequencing. Under Cd stress, DHZX exhibited significant decreases in photosynthetic pigments and increases in MDA, whereas neither changed significantly in YZ21C. Notably, despite the leaf Cd concentration in YZ21C being 2.6-fold higher than that of DHZX, YZ21C showed no more severe physiological damage, indicating stronger tissue-level Cd tolerance. Transcriptome sequencing identified 12,612 and 12,309 differentially expressed genes (DEGs) in YZ21C and DHZX, respectively, with sequencing reliability confirmed by qRT-PCR. Kyoto Encyclopedia of Genes and Genomes (KEGG) enrichment analysis showed that the comparison-specific DEGs in YZ21C were mainly enriched in defense-related pathways, including mitogen-activated protein kinase (MAPK) signaling, glutathione metabolism, and flavonoid biosynthesis, whereas the comparison-specific DEGs in DHZX were enriched in metabolic pathways such as fatty acid degradation and the citrate cycle (TCA cycle). In this study, a high Cd-tolerance material (YZ21C) and a Cd-sensitive material (DHZX) were selected, and KEGG enrichment analysis provided preliminary insight into their transcriptomic responses to Cd stress. These findings provide material resources and a theoretical basis for cultivation in Cd-contaminated areas, Cd-tolerant breeding, and further mining of key genes.

Keywords: *Lagerstroemia indica*; Cd stress; PCA; membership function; transcriptome; KEGG enrichment

Check for updates

Academic Editor: Othmane Merah

Received: 15 October 2026
Revised: 12 November 2026
Accepted: 13 November 2026
Published: 16 November 2026

Copyright: © 2026 by the authors. Licensee MDPI, Basel, Switzerland. This article is an open access article distributed under the terms and conditions of the Creative Commons Attribution (CC BY) license.

1. Introduction

Cadmium (Cd) is a widespread environmental heavy metal characterized by high toxicity and non-degradability. It can persist in soil and accumulate along the food chain, posing a threat to human health [1]. Approximately 9% of agricultural soils worldwide have Cd concentrations exceeding the relevant thresholds, with Cd exhibiting the highest exceedance rate among seven heavy metals and metalloids [2]. In China, the over-standard rate of Cd at soil monitoring points has reached 7.0%. Soil Cd contamination in regions such as the Yangtze River Delta, the Pearl River Delta, and areas surrounding mining districts has become a major constraint on land use and landscaping [3]. Given that the remediation of Cd-contaminated soils is time-consuming, costly, and often constrained by site conditions [4,5], it is of great practical significance to screen and utilize plants with strong adaptability and relatively high Cd tolerance for vegetation restoration and ecological greening [6]. In this context, landscape plants, which are generally not directly consumed, can reduce the risk of Cd transfer through the food chain while providing greening, beautification, and ecological restoration functions, making them promising materials for vegetation restoration in contaminated sites [7]. Therefore, screening Cd-tolerant landscape plants suitable for growth in Cd-contaminated areas is fundamental to the ecological restoration and landscape construction of contaminated sites.

Cd stress disrupts cellular redox homeostasis in plants, leading to excessive accumulation of reactive oxygen species (ROS) and consequently causing oxidative damage, ionic imbalance, and metabolic disorder [8]. To counteract these toxic effects, plants activate antioxidant defense systems to scavenge excess ROS and accumulate osmolytes to maintain cellular osmotic homeostasis [9]. However, Cd tolerance varies among germplasm accessions within the same species, as reflected in physiological responses such as growth, photosynthesis, and antioxidant defense. These differences can, to some extent, reflect Cd tolerance, and thus these physiological indicators are commonly used for tolerance evaluation [10]. On this basis, principal component analysis combined with the membership function method is commonly used to comprehensively evaluate multiple physiological indicators, and such methods have been widely applied in screening stress-tolerant germplasm [11,12]. Cd concentrations in different organs, together with the bioconcentration factor (BAF) and translocation factor (TF), can be used to compare Cd uptake and distribution among plant materials. However, these measurements alone do not explain the molecular basis of differences in Cd tolerance. Transcriptome sequencing can identify differentially expressed genes (DEGs) under Cd stress and, through KEGG enrichment analysis, reveal the associated regulatory pathways, thereby providing insights into the mechanisms of Cd tolerance in plants [13]. Previous studies have shown that differentially expressed genes in plants responding to Cd stress are often enriched in pathways such as antioxidant defense, glutathione metabolism, and phenylpropanoid biosynthesis [14–16]. However, pathway enrichment does not necessarily equate to a key role. Therefore, integrating physiological responses and organ-specific Cd distribution with transcriptomic data, supported by qRT-PCR validation, may help explain differences in Cd tolerance among germplasms [17,18].

Crape myrtle (*Lagerstroemia indica* L.) is a deciduous shrub or small tree belonging to the genus *Lagerstroemia* in the family Lythraceae. It is characterized by a long flowering period, abundant blooms, and strong adaptability [19]. As an important summer-flowering ornamental species, crape myrtle is widely used in urban landscapes and park design [20]. The genus *Lagerstroemia* is rich in germplasm resources, with more than 50 species worldwide; China harbors 24 wild species and over 350 cultivated varieties [21,22]. Crape myrtle has also shown preliminary potential for adaptation to heavy metal-contaminated environments. A three-year vegetation screening trial in a copper mining area showed that, among

21 tested tree species, crape myrtle achieved a survival rate of 100% [23]. Another study found that crape myrtle has a certain capacity for Cd accumulation, with Cd predominantly accumulated in roots and relatively lower contents in aboveground parts, indicating its potential for application in Cd-contaminated areas [24]. However, existing studies have mainly focused on a limited number of crape myrtle materials, and systematic comparisons of Cd tolerance among different germplasm accessions remain scarce. Moreover, the differences in their growth performance, physiological responses, and molecular regulation have not been fully elucidated. This, to some extent, has limited the application of elite Cd-tolerant crape myrtle germplasm.

In this context, different crape myrtle germplasm accessions were systematically compared in terms of their growth phenotypes and physiological responses under Cd stress. Multiple growth and physiological indicators were measured, and Cd tolerance was comprehensively evaluated using principal component analysis combined with the membership function method. Cd-tolerant and Cd-sensitive accessions were then selected for further analysis. Subsequently, rooted cuttings were obtained through cutting propagation, and physiological indicators were measured to verify the stability of Cd-tolerant phenotypes. In addition, Cd concentrations in the roots, stems, and leaves were measured, and the bioconcentration factor (BAF) and translocation factor (TF) were calculated to compare Cd accumulation and organ-specific distribution between the two types of accessions. On this basis, transcriptome sequencing was performed on the rooted cuttings, and combined with KEGG pathway enrichment analysis, regulatory pathways related to Cd tolerance were explored, and qRT-PCR was used to validate the reliability of the transcriptome data. This study aimed to reveal the differences in physiological responses, organ-specific Cd distribution characteristics, and transcriptional regulation features of Cd tolerance among different crape myrtle germplasm accessions, providing a reference for the study of Cd tolerance mechanisms in woody plants, and a theoretical basis for the screening of Cd-tolerant crape myrtle germplasm and its application in Cd-contaminated soils.

2. Results

2.1. Effects of Cd Stress on Growth Phenotype and Photosynthetic Pigments

To investigate the growth and photosynthetic responses of crape myrtle to Cd stress, seedlings were treated with 3000 μmol L^{-1} $CdCl_2$, and growth traits and photo-synthetic pigment contents were measured. The results showed that Cd stress inhibited seedling growth and photosynthetic pigment accumulation, with the magnitude of these effects varying among materials. Overall, Cd-treated seedlings showed reduced stature and leaf yellowing, with some also exhibiting shortened and browned roots (Figure 1a). Plant height decreased in most materials, most markedly in No. 24, whereas Nos. 7, 8, 12, 18, and 21 showed only minor, non-significant changes relative to controls (Figure 1b). These results indicate that aboveground growth sensitivity to Cd stress varies among materials. Compared with plant height, root length varied more among materials under Cd stress. Root length decreased in most seedlings, most strongly in No. 8, but increased in a few materials, most notably in No. 24, followed by Nos. 11 and 20 (Figure 1c). Overall, Cd stress inhibited the growth of crape myrtle seedlings, with Cd tolerance varying among materials. Total photosynthetic pigment contents generally decreased under Cd stress, but pigment retention differed among materials (Figure 1d,e). Chlorophyll b was more sensitive to Cd stress than chlorophyll a and showed a greater overall decrease (Figure 1e). Pigment inhibition was strongest in No. 4, with chlorophyll a, chlorophyll b, and carotenoid contents reduced by 51.0%, 72.1%, and 52.5%, respectively. In Nos. 2 and 3, chlorophyll b content decreased by more than 75% (Figure 1e). In contrast, chlorophyll a content remained relatively stable in Nos. 7, 11, 14, and 20 (Figure 1d), whereas Nos. 12 and 21 maintained

chlorophyll b content more effectively. In addition, carotenoid content increased after Cd treatment in Nos. 6, 16, and 17, with the greatest increase observed in No. 16 (Figure 1f). Overall, Cd stress inhibited photosynthetic pigment synthesis and accumulation in crape myrtle, although some materials maintained pigment levels better than others.

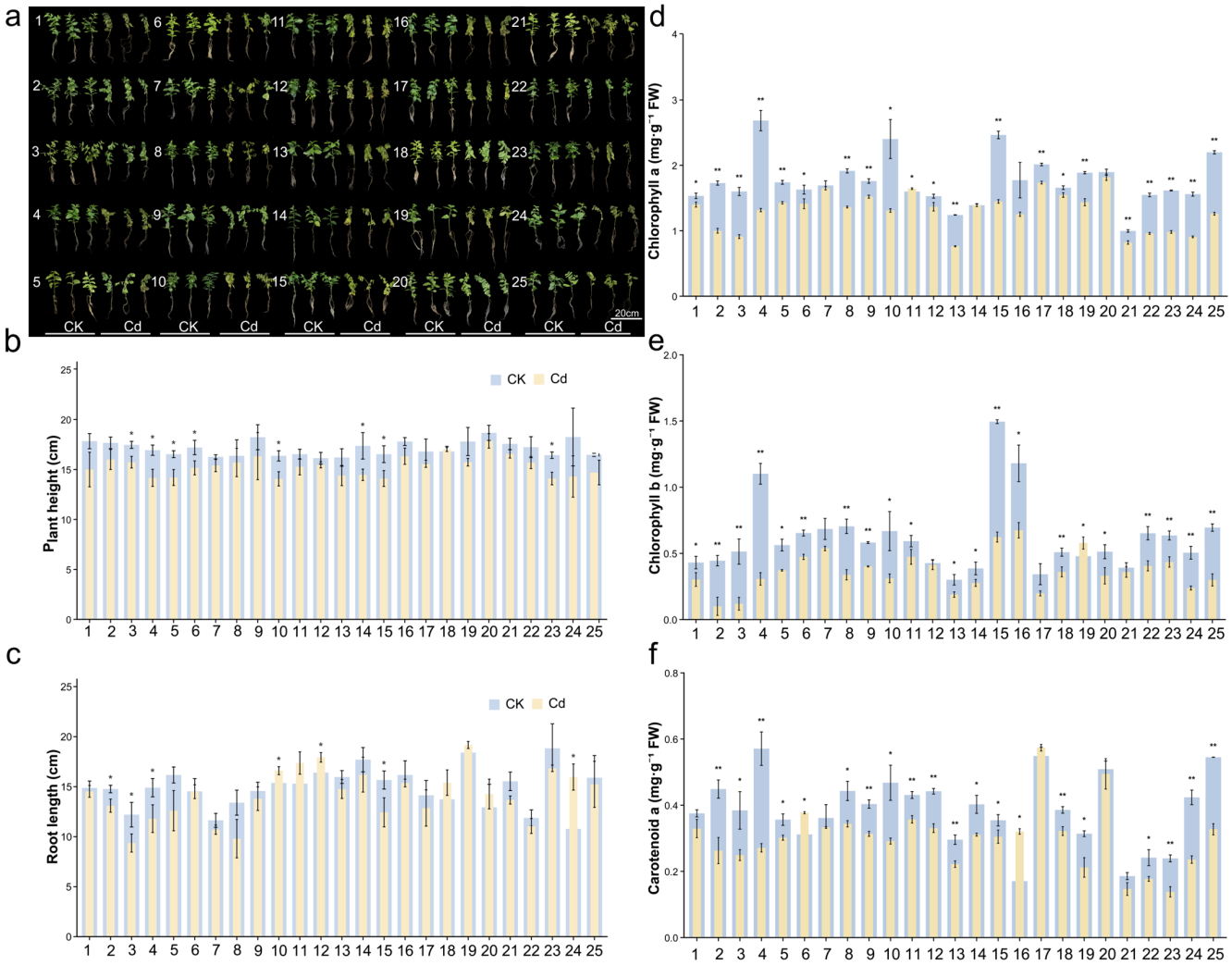


Figure 1. Effects of Cd stress on growth phenotype, plant height, root length, and photosynthetic pigment contents in 25 crape myrtle materials. (**a**) Representative images of the 25 crape myrtle materials under control (CK) and Cd treatments. For each numbered material, the three plants on the left are CK-treated, and the three on the right are Cd-treated. Scale bar = 20 cm. (**b**) Plant height. (**c**) Root length. (**d**) Chlorophyll a content. (**e**) Chlorophyll b content. (**f**) Carotenoid content. Numbers 1–25 indicate the 25 crape myrtle materials. In panels (**b**–**f**), the blue bars represent the control (CK) group, and the yellow bars represent the Cd treatment group. Data are presented as the mean ± standard deviation ($n = 3$ biological replicates). * $p < 0.05$; ** $p < 0.01$. Differences without asterisks are not significant ($p > 0.05$).

2.2. Effects of Cd Stress on Antioxidant Defense and Membrane Lipid Peroxidation

Antioxidant enzyme activities and the contents of osmotic adjustment substances and malondialdehyde (MDA) were measured in 25 crape myrtle materials to characterize their antioxidant defense, osmotic regulation, and membrane lipid peroxidation responses to Cd stress and to identify differences among materials. Cd stress affected the physiological defense system, with response patterns varying among materials. Cd stress altered antioxidant enzyme activities in crape myrtle, with distinct responses among enzymes. Specifically,

after Cd treatment, peroxidase (POD) activity increased significantly in Nos. 1, 6, and 7 but was inhibited in Nos. 9, 11, and 14 (Figure 2a). Superoxide dismutase (SOD) activity increased most in Nos. 1, 19, and 20, whereas it was weak or inhibited in Nos. 8, 9, and 10 (Figure 2b). Catalase (CAT) activity increased significantly in Nos. 1, 3, and 8 but decreased significantly in Nos. 4, 7, and 12 (Figure 2c). Overall, the activities of the three antioxidant enzymes increased coordinately in Nos. 1, 2, 6, 18, and 25, with No. 1 exhibiting highly significant increases in all three. The osmotic adjustment and lipid peroxidation responses to Cd stress varied among materials; proline (PRO) content increased in all materials, with highly significant increases in most (Figure 2d). PRO accumulation varied markedly among materials, with the highest content in No. 12. Soluble protein (SP) content showed two distinct response patterns to Cd stress (Figure 2e): it increased significantly in materials such as Nos. 1, 2, and 6, but showed a decreasing trend in Nos. 4, 9, and 12. Changes in MDA content indicated that membrane lipid peroxidation increased in most materials after Cd treatment, with highly significant increases in Nos. 1, 7, and 9, whereas MDA content in materials such as Nos. 3, 4, and 5 did not differ significantly from that in the control (Figure 2f).

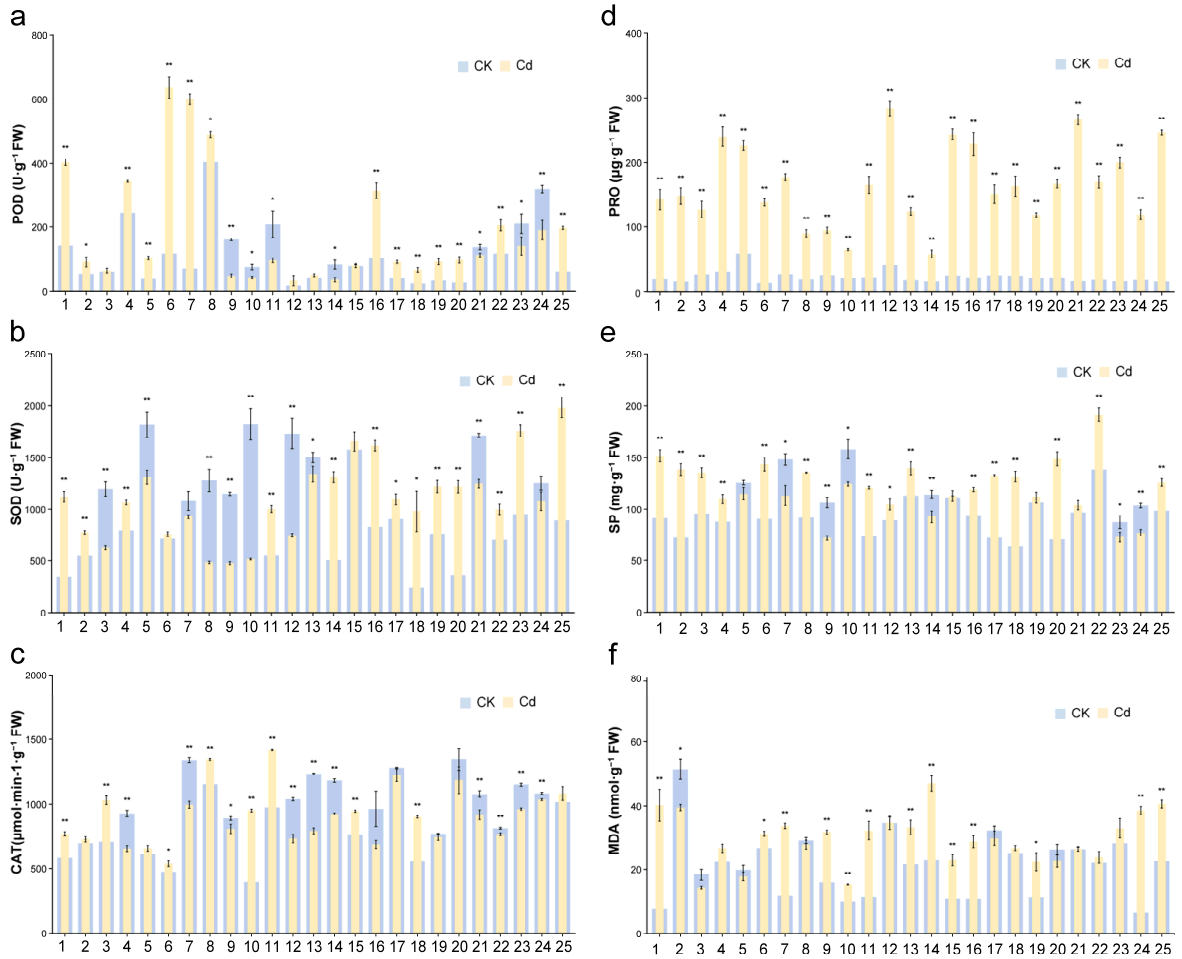


Figure 2. Effects of Cd stress on antioxidant enzyme activities and physiological responses in crape myrtle. (**a**) POD activity; (**b**) SOD activity; (**c**) CAT activity; (**d**) PRO content; (**e**) SP content; and (**f**) MDA content. CK, control; Cd, cadmium treatment. Nos. 1–25 represent the 25 tested materials. Data are presented as mean ± standard deviation ($n = 3$ biological replicates). Statistical analysis was performed as described in Figure 1. * $p < 0.05$, ** $p < 0.01$; no asterisk indicates no significant difference ($p > 0.05$).

2.3. Correlation Analysis of Indicators and Comprehensive Evaluation of Cd Tolerance

To assess the relationships among growth and physiological traits in crape myrtle under Cd stress and characterize their coordinated responses, correlation analysis was performed on the tolerance indices (Table S1) for growth traits, photosynthetic pigments, antioxidant enzyme activities, and osmotic adjustment traits (Figure 3). Some associations were observed between growth and physiological traits under Cd stress, although correlations among most traits were weak. Within the photosynthetic pigment system, chlorophyll a, chlorophyll b, and carotenoids were all positively correlated, indicating coordinated changes in photosynthetic pigments under Cd stress. Plant height was positively correlated with chlorophyll content, suggesting that the maintenance of photosynthetic capacity may benefit aboveground growth. In contrast, root length was weakly correlated with most physiological traits, indicating that root growth may respond differently from aboveground growth. Within the antioxidant system, SOD activity was positively correlated with SP content, suggesting their joint contribution to oxidative damage responses and osmotic regulation under Cd stress. Overall, Cd tolerance in crape myrtle cannot be assessed reliably by a single trait but should be evaluated comprehensively using multiple traits, including growth, photosynthetic pigments, the antioxidant system, and membrane lipid peroxidation.

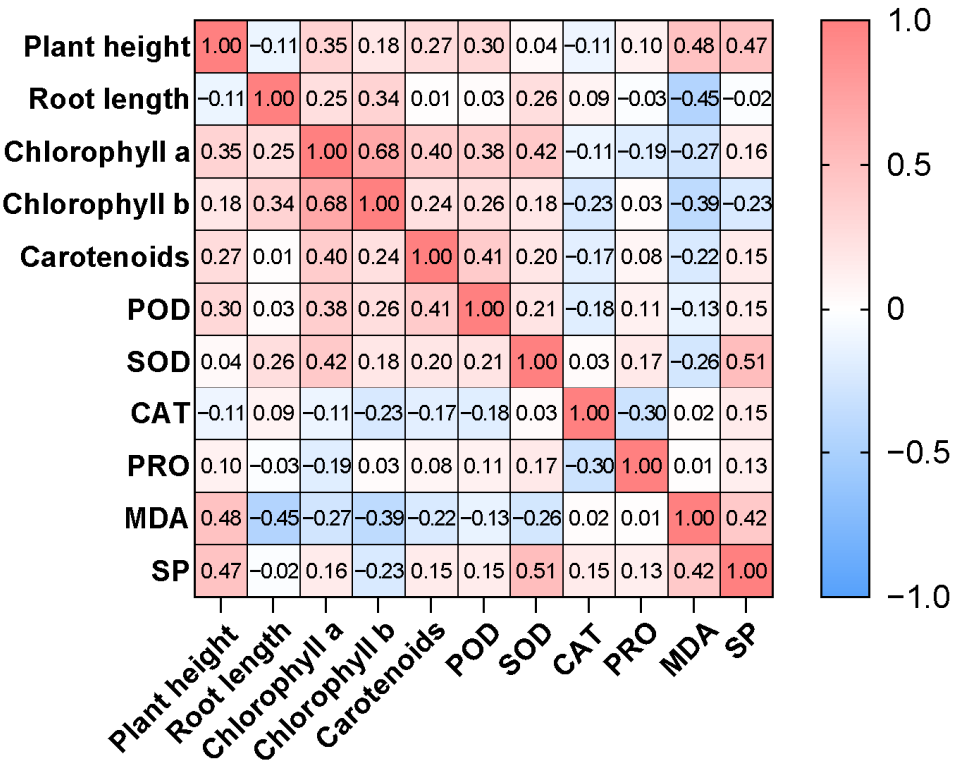


Figure 3. Pearson correlation heatmap of growth and physiological traits. The color scale ranges from −1 to 1, with blue indicating negative correlations and red indicating positive correlations. POD, peroxidase; SOD, superoxide dismutase; CAT, catalase; PRO, proline; MDA, malondialdehyde; SP, soluble protein.

To systematically evaluate differences in Cd tolerance among 25 crape myrtle materials and select representative materials for subsequent physiological and transcriptomic analyses, principal component analysis (PCA) was performed on the tolerance index (TI) values of 11 indicators. Six principal components (PCs) were extracted, cumulatively explaining 84% of the total variance (Table S3). Based on these six PCs, the membership function method was used to calculate a comprehensive Cd-tolerance value (D value) for each material. The

D values ranged from 0.321 to 0.793 (Table S2), with material No. 20 having the highest value (0.793) and material No. 9 the lowest (0.321). Based on the D values, hierarchical cluster analysis was performed using Euclidean distance and the average-linkage method, classifying the 25 materials into four groups: highly Cd-tolerant, Cd-tolerant, moderately Cd-tolerant, and Cd-sensitive (Figure 4a). A two-dimensional PCA score plot was then generated using the two PCs with the greatest contributions (PC1 and PC2; Figure 4b). The four groups showed some degree of clustering and separation, and their overall distribution was generally consistent with the clustering results. The High Cd-tolerance group had higher SOD and POD activities and accumulated more PRO and SP, indicating stronger antioxidant and osmotic adjustment capacities. By contrast, the Cd-sensitive group showed lower photosynthetic pigment contents and antioxidant enzyme activities, together with higher MDA content, consistent with more severe membrane lipid peroxidation. Based on the comprehensive evaluation, rooted cuttings of No. 20 (YZ21C; highly Cd-tolerant) and No. 9 (DHZX; Cd-sensitive) were selected as experimental materials. After Cd stress treatment, their physiological parameters and organ-specific Cd accumulation and distribution were assessed. Furthermore, transcriptome sequencing was combined with qRT-PCR validation to elucidate the physiological responses and molecular basis underlying their differential Cd tolerance.

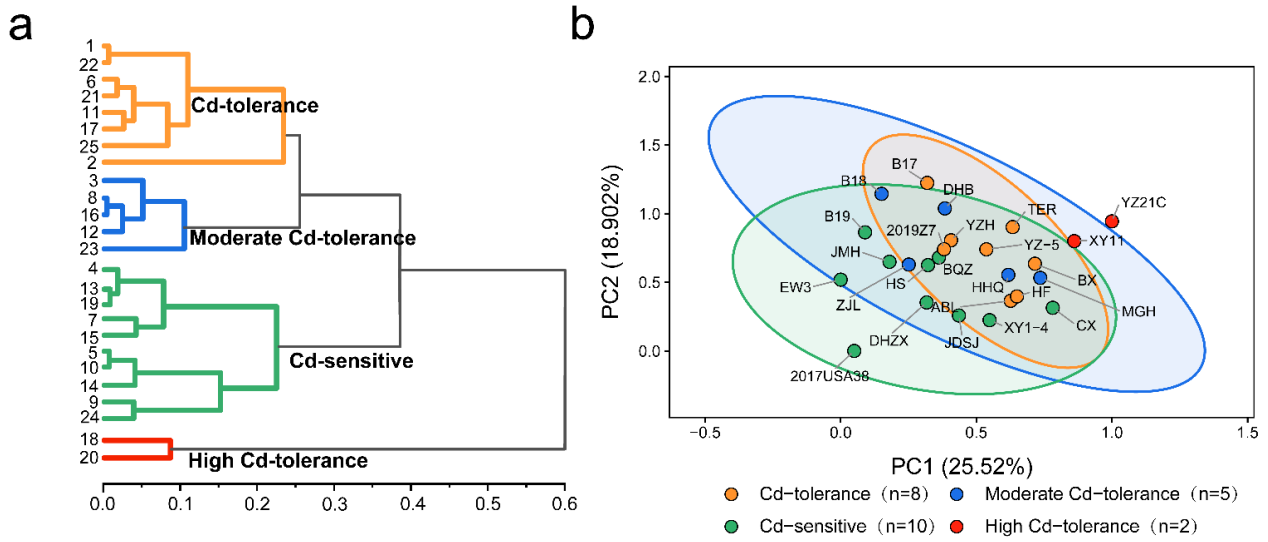


Figure 4. Hierarchical clustering and principal component analysis. (**a**) Cluster dendrogram based on Euclidean distance. (**b**) Principal component analysis based on 11 physiological traits. PC1 and PC2 explained 25.53% and 18.92% of the variance, respectively. The red, blue, green, and orange colors in the dendrogram branches and the circles in panel (**b**) represent the High Cd-tolerance, Moderate Cd-tolerance, Cd-sensitive, and Cd-tolerance groups, respectively.

2.4. Effects of Cd Stress on Growth and Physiological Characteristics of Cd-Tolerant and Cd-Sensitive Crape Myrtle

To validate the reliability of the screening results obtained at the seedling stage, rooted cuttings of Cd-tolerant material YZ21C and Cd-sensitive material DHZX were subjected to Cd stress. Following Cd stress, growth was inhibited to varying degrees in both materials, with more severe symptoms in the Cd-sensitive material DHZX. The leaves of DHZX showed chlorosis, wilting, and abscission, whereas YZ21C exhibited only slight wilting (Figure 5a). These observations were consistent with the results of the seedling-stage screening. Further measurements showed that, following Cd stress, total chlorophyll content decreased in both materials, but the decrease was significantly smaller in YZ21C than in DHZX (Figure 5b). In YZ21C, neither carotenoid nor MDA content changed significantly relative to the con-

trol (Figure 5c,d), whereas DHZX showed significant decreases in total chlorophyll and carotenoid contents and a significant increase in MDA content (Figure 5b–d). These changes were consistent with the phenotypic differences, indicating greater damage to the photosynthetic apparatus and more extensive membrane lipid peroxidation in DHZX than in YZ21C.

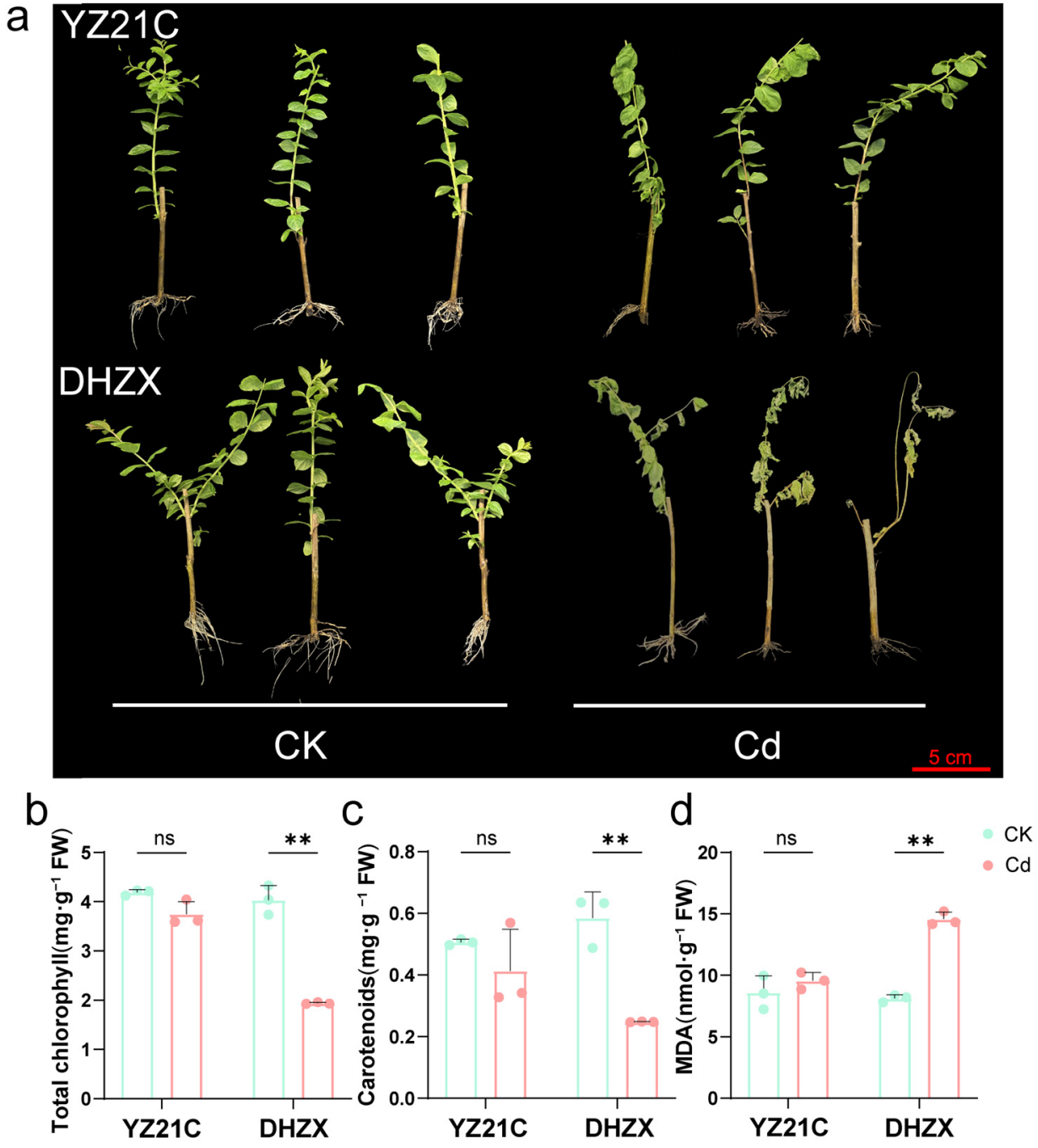


Figure 5. Growth phenotypes and physiological analyses of rooted cuttings of the Cd-tolerant and Cd-sensitive materials under Cd stress. (**a**) Phenotypes of rooted cuttings of the Cd-tolerant (YZ21C) and Cd-sensitive (DHZX) materials under control (CK) and Cd treatment conditions (scale bar = 5 cm). (**b**) Total chlorophyll content (mg·g^{-1} FW). (**c**) Carotenoid content (mg·g^{-1} FW). (**d**) MDA content (nmol·g^{-1} FW). Data are presented as the mean ± standard deviation (n = 3). Asterisks indicate significant differences between the Cd-treated and control groups within the same accession ($p < 0.01$); ns indicates no significant difference.

2.5. Transcriptome Analysis of Cd-Tolerant and Cd-Sensitive Crape Myrtle Under Cd Stress

To compare Cd accumulation and organ distribution between the two crape myrtle materials under Cd stress, Cd concentrations were measured in the roots, stems, and leaves, and the bioaccumulation factor (BAF) and translocation factor (TF) were calculated. In both materials, Cd concentrations were highest in the roots, followed by the stems and leaves (Figure 6a). Under Cd treatment, Cd concentrations in the roots and leaves of YZ21C were approximately 2.6-fold those in DHZX, whereas the concentration in the stems was approximately 1.45-fold that in DHZX (Figure 6a). The organ-wise distribution of BAF was generally consistent with that of Cd concentrations (Figure 6b). TF analysis showed that the $TF_{leaf/root}$ was similar between the two materials, whereas the $TF_{stem/root}$ was higher in DHZX than in YZ21C, indicating a greater relative translocation of Cd from roots to stems in DHZX (Figure 6c). Notably, compared with their respective controls, photosynthetic pigment and MDA contents in YZ21C leaves were not significantly affected by Cd treatment. In contrast, these parameters changed significantly in DHZX leaves, despite their lower Cd concentration. To further investigate the transcriptional responses underlying these physiological differences, leaf samples from both materials underwent transcriptome sequencing.

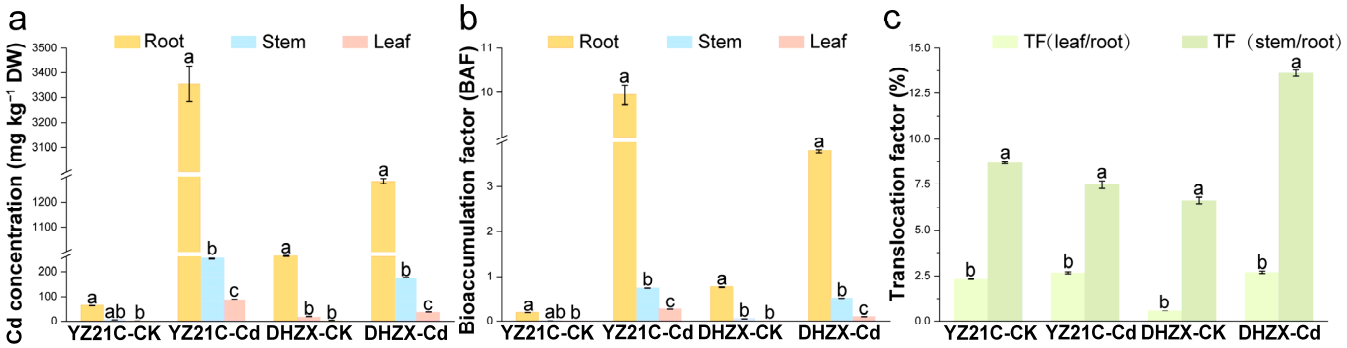


Figure 6. Cd accumulation and translocation in Cd-tolerant and Cd-sensitive crape myrtle under Cd stress. (**a**) Cd concentrations in roots, stems, and leaves (mg kg^{-1} DW) (**b**) Bioaccumulation factor (BAF) in different organs. (**c**) Translocation factors (TF, %) from roots to stems ($TF_{leaf/root}$) and from roots to leaves ($TF_{stem/root}$) Data are presented as mean ± standard deviation (SD) ($n = 3$). Different lowercase letters indicate significant differences among organs within the same treatment (Tukey's HSD test, $p < 0.05$). Broken y-axes are used in panels (**a**,**b**); omitted intervals are 260–900 and 1300–3000 in (**a**), and 3–10 in (**b**). CK, control; Cd, cadmium treatment.

2.6. Transcriptomic Analysis and qRT-PCR Validation of Cd-Tolerant and Cd-Sensitive Crape Myrtle Under Cadmium Stress

To investigate the transcriptional regulatory mechanisms underlying the response of crape myrtle to Cd stress, leaf samples from CK and Cd treatments were subjected to RNA sequencing. After quality control, approximately 44.2 million clean reads were obtained from the 12 samples. All samples had Q20 ≥ 99.4%, Q30 ≥ 97.6%, and GC content of 49.54–50.23%, indicating consistently high sequencing quality. More than 90% of the clean reads mapped to the crape myrtle reference genome, indicating good sequencing accuracy and mapping efficiency and meeting the requirements for subsequent identification of differentially expressed genes and functional enrichment analysis (Table S4). Under Cd stress, 12,612 DEGs were identified in YZ21C relative to its respective control (Table S5), including 8957 upregulated and 3655 downregulated genes. In DHZX, 12,309 DEGs were identified relative to its respective control (Table S6), including 8023 upregulated and 4286 downregulated genes (Figure 7a). PCA revealed clear separation among the four sample groups, with biological replicates clustering closely within each group, indicating high

reproducibility and distinct transcriptional profiles between groups (Figure 7b). Biological replicates within each group showed high consistency, with correlation coefficients all above 0.99, whereas between-group correlations were generally lower (Figure S1). Venn diagram analysis identified 5746 Y-comparison-specific DEGs and 5443 D-comparison-specific DEGs (Figure 7c). Scatter-plot analysis of the 6866 shared DEGs revealed that most genes exhibited concordant expression changes in both materials (i.e., up- or downregulated in both), whereas a small subset showed opposite trends (Figure S2; Table S7). KEGG enrichment analysis showed that DEGs shared by YZ21C and DHZX were enriched in photosynthesis, plant hormone signal transduction, phenylpropanoid biosynthesis, and starch and sucrose metabolism, representing common transcriptional features of crape myrtle under Cd stress. Y-comparison-specific DEGs were mainly enriched in defense-related pathways, including glutathione metabolism, the plant MAPK signaling pathway, flavonoid biosynthesis, peroxisome, and arginine and proline metabolism. In contrast, D-comparison-specific DEGs were mainly enriched in metabolic pathways, including phenylpropanoid biosynthesis, fatty acid degradation, and the citrate cycle (TCA cycle) (Figure 7d; Table S8). These differences in pathway enrichment were consistent with the physiological responses of the two materials. In YZ21C, the enrichment of defense-related pathways may be associated with the relatively limited physiological changes observed under Cd stress, including the absence of a significant increase in MDA content and relatively small changes in photosynthetic pigment levels. In contrast, the enrichment of metabolic pathways among D-comparison-specific DEGs suggests transcriptional responses involving lipid, energy, and secondary metabolism. To validate the RNA-seq results, qRT-PCR analysis was performed on 10 randomly selected differentially expressed genes using *LiEF-1α* as the reference gene. These genes were primarily associated with glutathione metabolism, antioxidant defense, and NADPH supply, and their expression patterns were broadly consistent with the RNA-seq results (Table S9). Under control (CK) conditions, the expression levels of these genes were similar between the two materials. Under Cd stress, all 10 genes were significantly upregulated in YZ21C. In DHZX, *APX2*, *GSTU8*, *PGD3*, *GSTF11*, and *PGD2* were significantly downregulated, whereas *IDH1* showed no significant change. These results indicate that Cd stress significantly upregulated the expression of the tested genes in YZ21C, whereas several genes were downregulated in DHZX.

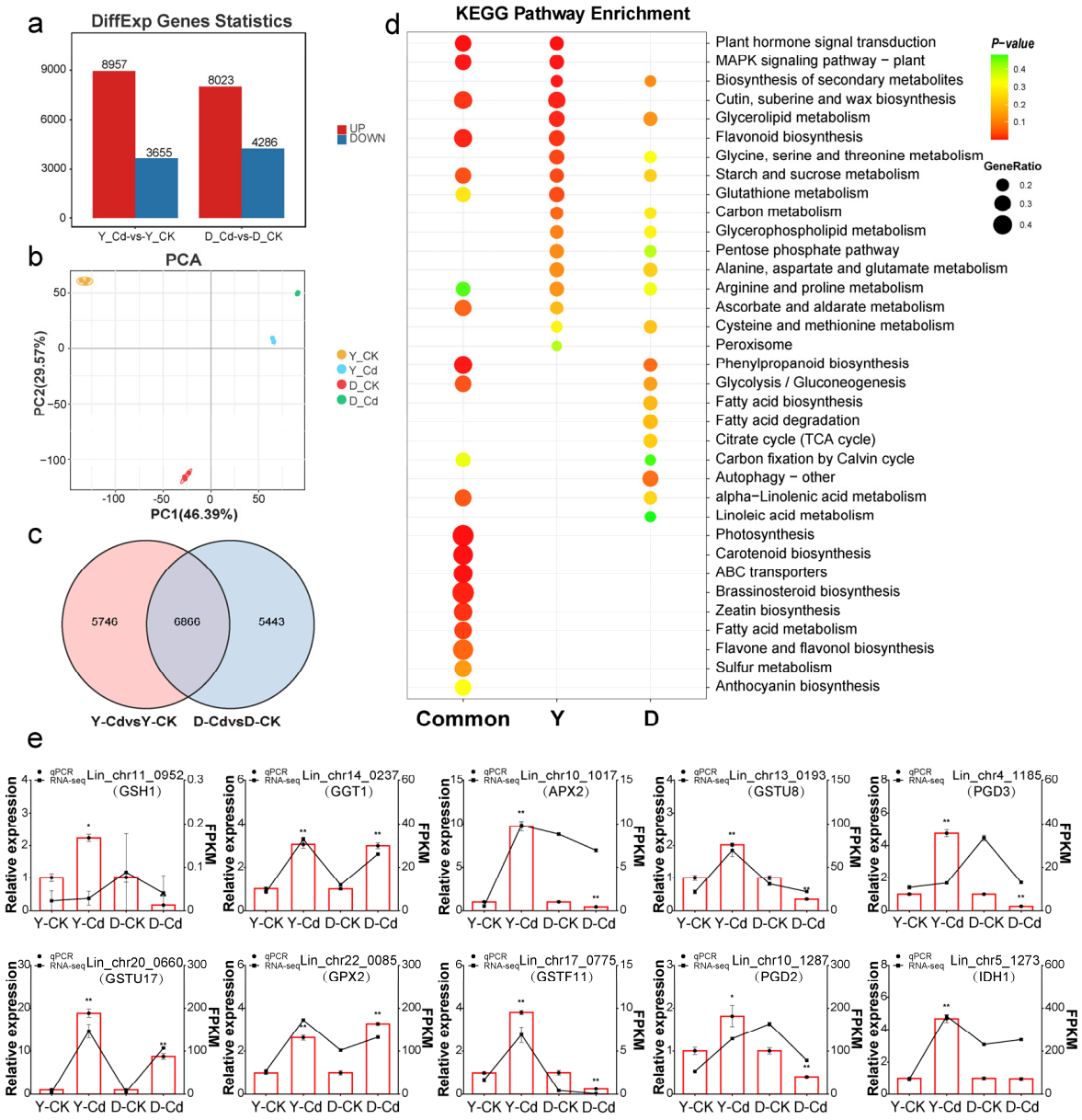


Figure 7. Transcriptomic analysis and qRT-PCR validation of rooted cuttings from Cd-tolerant (YZ21C) and Cd-sensitive (DHZX) materials under Cd stress. (**a**) Numbers of upregulated (red) and downregulated (blue) DEGs. (**b**) PCA of transcriptomic profiles. (**c**) Venn diagram showing shared and comparison-specific DEGs. (**d**) KEGG pathway enrichment of DEGs. Bubble size indicates GeneRatio; color indicates *p*-values (red, lower; green, higher). "Common" denotes DEGs shared by YZ21C and DHZX; "Y" and "D" denote comparison-specific DEGs in YZ21C and DHZX, respectively. (**e**) qRT-PCR validation of 10 candidate DEGs. Red bars show relative expression levels (left *y*-axis), and black lines show RNA-seq FPKM values (right *y*-axis); note the different scales. Data are means ± SD ($n = 3$ biological replicates). Asterisks indicate significant differences between Cd-treated and control groups within each material (* $p < 0.05$; ** $p < 0.01$; Student's *t*-test).

3. Discussion

3.1. Physiological Responses and Evaluation of Cd Tolerance in Crape Myrtle Under Cd Stress

This study combined physiological assessments, Cd accumulation/distribution analyses, and transcriptomic profiling to investigate the physiological and transcriptional mechanisms of Cd tolerance in crape myrtle materials. For effective screening, the stress intensity must induce clear symptoms without causing lethal damage that masks genotypic differ-

ences [25]. Our preliminary gradient test revealed that lower Cd doses caused only mild symptoms, whereas higher doses caused severe damage. Thus, 3000 μmol L^{-1} $CdCl_2$ for 7 days was selected as an appropriate treatment condition [26]. Hydroponic culture helped ensure uniform nutrient and Cd exposure while minimizing soil interference [27]. Following Cd treatment, we assessed phenotypic and physiological traits and used membership function analysis combined with principal component analysis to identify No. 20 (YZ21C) as the Cd-tolerant material and No. 9 (DHZX) as the Cd-sensitive material. Under Cd stress, crape myrtle seedlings generally exhibited plant dwarfing and leaf chlorosis, while some also showed root shortening and browning. However, the severity of these responses varied among materials, and changes in aboveground and belowground growth were not entirely consistent. For example, No. 8 did not differ significantly from the control in plant height but showed the greatest reduction in root length. In contrast, No. 24 exhibited the strongest inhibition of plant height, whereas its root length increased compared with the control. These results indicate that different organs within the same material may differ in their sensitivity to Cd stress and that increased root length does not necessarily indicate greater overall Cd tolerance [28]. Therefore, changes in plant height or root length alone are insufficient to fully assess Cd tolerance among crape myrtle materials. Damage to the photosynthetic apparatus is one of the major factors contributing to growth inhibition under Cd stress [29]. In this study, photosynthetic pigment contents decreased after Cd treatment in most crape myrtle materials, with the overall reduction in chlorophyll b content being greater than that in chlorophyll a content. This suggests that chlorophyll b was more sensitive to Cd stress [30]. In addition, crape myrtle materials differed in their ability to maintain photosynthetic pigments under Cd stress. Chlorophyll a or chlorophyll b content remained relatively stable in some materials, whereas carotenoid content increased in others. The relative stability of chlorophyll content may help maintain light absorption, whereas increased carotenoid content may be associated with photoprotection and antioxidant defense [31]. These findings suggest that crape myrtle materials may respond to Cd stress through differential regulation of photosynthetic pigments. Antioxidant defense is an important mechanism by which plants mitigate Cd-induced oxidative damage [32,33]. In this study, relative to the control, the activities of POD, SOD, and CAT varied markedly among crape myrtle materials and enzyme types. Some materials showed coordinated increases in all three enzyme activities, whereas others showed inconsistent changes, with the activities of different enzymes changing in different directions. These results indicate that the antioxidant response of crape myrtle to Cd stress is not governed by a single enzyme system [34]. PRO, SP, and MDA contents showed different patterns of response to Cd stress. PRO content increased significantly in all tested materials, indicating that PRO accumulation was a common response to Cd stress among the crape myrtle materials examined in this study. In contrast, SP and MDA contents showed material-dependent increases or decreases [35]. For example, in material No. 14, Cd stress significantly increased PRO and MDA contents but significantly decreased SP content, indicating that PRO accumulation occurred concurrently with increased membrane lipid peroxidation. Therefore, increased PRO content alone cannot be taken as evidence of enhanced Cd tolerance [36]. Notably, simultaneous increases in multiple defense-related indicators do not necessarily indicate reduced membrane lipid peroxidation. In material No. 1, Cd stress significantly increased POD, SOD, and CAT activities, as well as PRO and SP contents; however, MDA content also increased significantly. These results indicate that increases in defense-related indicators can coexist with increased membrane lipid peroxidation. Thus, increases in antioxidant enzyme activities, PRO content, or SP content alone are insufficient to demonstrate enhanced Cd tolerance in crape myrtle, highlighting the need to evaluate defense responses alongside indicators of stress-induced damage [37]. In summary, Cd tolerance in crape myrtle is multifaceted,

involving growth maintenance, photosynthetic pigment regulation, antioxidant defense, osmotic adjustment, and membrane lipid peroxidation. These physiological processes are interrelated but do not always change in the same direction. A single indicator reflects only one physiological process or damage state and is therefore insufficient to distinguish the adaptive activation of defense mechanisms from stress-induced injury or to capture differences among organs and physiological processes. Therefore, integrating multiple indicators into a comprehensive evaluation can reduce the limitations of single-indicator assessment and improve the reliability of screening for Cd-tolerant germplasm [38]. In this study, PCA was used to extract the principal components, and membership function analysis was then applied to these components to calculate a composite evaluation value. This approach integrates growth performance, physiological defense, and the extent of injury across materials, providing a basis for comparing and screening Cd-tolerant crape myrtle germplasm. Based on the composite evaluation, No. 20 was identified as Cd-tolerant (YZ21C), whereas No. 9 was identified as Cd-sensitive (DHZX).

3.2. Physiological Responses and Cd Accumulation and Partitioning Associated with Differential Cd Tolerance in Crape Myrtle

Rooted cuttings of YZ21C and DHZX, identified through preliminary screening, were used to verify the stability of their contrasting Cd-tolerance phenotypes. Physiological parameters were measured, and Cd accumulation and partitioning were analyzed to compare their responses to Cd stress. The growth responses of the rooted cuttings were broadly consistent with those observed in seedlings, indicating that the difference in Cd tolerance between the two materials was reproducible under the conditions tested. Under Cd stress, photosynthetic pigment contents decreased significantly and MDA content increased significantly in DHZX, whereas neither parameter changed significantly in YZ21C. These responses were consistent with the contrasting tolerance phenotypes, suggesting that the maintenance of photosynthetic pigments and limitation of lipid peroxidation may be associated with Cd tolerance in crape myrtle. Both materials preferentially accumulated Cd in their roots, consistent with reports for other woody species, including *Rhododendron pulchrum* [39] and *Populus* spp. [40]. Although YZ21C had a lower $TF_{stem/root}$ than DHZX, its stem and leaf Cd concentrations were higher. Thus, its greater Cd tolerance cannot be explained solely by its lower $TF_{stem/root}$. Despite its higher leaf Cd concentration, YZ21C did not exhibit more pronounced physiological damage. This suggests that the difference in tolerance between the two materials cannot be explained solely by total tissue Cd concentrations, which may also involve internal Cd tolerance and detoxification mechanisms. To investigate the potential molecular basis of this difference, leaf transcriptome analysis was performed to identify pathways and candidate genes associated with their contrasting Cd tolerance.

3.3. Transcriptional Response Features of Differential Cd Tolerance in Crape Myrtle

Transcriptomic analysis revealed distinct responses to Cd stress in the two materials. Although the numbers of differentially expressed genes (DEGs) were similar, the enriched pathways differed. Shared DEGs were enriched in photosynthesis, plant hormone signal transduction, and starch and sucrose metabolism, which are associated with light-energy use [41,42], stress signaling [43], and energy metabolism [44], respectively. Similar responses have been reported in rice, Arabidopsis, and other species [45,46], suggesting that the two materials share some responses to Cd stress. In YZ21C, material-specific DEGs were enriched in MAPK signaling, glutathione metabolism, and flavonoid biosynthesis. MAPK cascades mediate stress signaling and regulate antioxidant defenses [47], while glutathione contributes to antioxidant protection and provides a precursor for phytochelatin synthesis, thereby supporting Cd chelation and vacuolar sequestration [48]. Flavonoids can also

scavenge reactive oxygen species as non-enzymatic antioxidants [49]. Cd concentrations in roots, stems, and leaves were higher in YZ21C than in DHZX, with the leaf Cd concentration approximately 2.6-fold that in DHZX. However, MDA and photosynthetic pigment contents in YZ21C did not differ significantly from those in the control (CK). These results suggest that enhanced transcriptional responses related to antioxidant defense and detoxification may help YZ21C maintain physiological stability despite greater Cd accumulation. By contrast, DHZX-specific DEGs were enriched in fatty acid degradation and the citrate cycle, potentially indicating lipid catabolism and compensatory energy metabolism following membrane damage [50]. This interpretation is consistent with the higher MDA content, lower photosynthetic pigment content, lower leaf Cd concentration, and higher $TF_{stem/root}$ observed in DHZX. Together, these results suggest that these metabolic changes may reflect Cd-induced damage and a compensatory response. The qRT-PCR results broadly agreed with the RNA-seq trends. All 10 genes associated with glutathione metabolism, antioxidant defense, or NADPH supply were significantly upregulated in YZ21C. In DHZX, five genes were significantly downregulated, while the other five showed no significant change. These results support differences in the transcriptional responses of defense-related genes between the two materials.

Overall, differences in Cd tolerance between the two materials may be related to organ-level Cd partitioning and translocation, as well as their transcriptional responses. By combining multi-index evaluation with physiological measurements, analyses of Cd accumulation and organ partitioning, and transcriptomic profiling, this study characterized the physiological and transcriptional responses of the materials to Cd stress. The findings provide a basis for further investigation of Cd tolerance mechanisms in crape myrtle, the selection of Cd-tolerant germplasm, and the evaluation of its potential for landscaping and vegetation restoration in Cd-contaminated areas. This study used high-concentration, short-term Cd exposure for rapid screening. The Cd tolerance and application potential of the candidate materials therefore require validation in soil and field trials. Further functional characterization of candidate genes is also needed to clarify the mechanisms underlying Cd tolerance.

4. Materials and Methods

4.1. Plant Materials

Twenty-five crape myrtle seedling materials, numbered 1–25, were used in this study. Mature seeds were collected in December 2025 from one mother tree of each of the 25 named crape myrtle cultivars. Details of the mother trees are provided in Table 1. All mother trees are maintained in the germplasm repository of the Zhejiang Academy of Forestry. For simplicity, the materials are referred to as Nos. 1–25 throughout the text and figures.

Table 1. Names of the 25 crape myrtle cultivars from which the mother trees were selected.

No.	Abbreviation	Cultivar Name	Geographic Distribution	Growth Form	No.	Abbreviation	Cultivar Name	Geographic Distribution	Growth Form
1	ABL	Apollo	United States	Tree	14	JDSJ	Juediao Shuangjiao	Hunan, China	Shrub
2	B17	L. I. Durant Red	United States	Tree	15	JMH	Jianmin Hong	Hunan, China	Tree
3	B18	L. Petit Orchid	United States	Tree	16	MGH	Meigui Hong	Jiangsu, China	Tree
4	B19	L. Petit Pink	United States	Tree	17	TER	Tian'e Rong	United States	Shrub
5	BQZ	Baoqing Zi	Hunan, China	Tree	18	XY11	Qianchao Xingbai	Zhejiang, China	Tree
6	BX	Baixue	Fujian, China	Tree	19	XY1-4	Chenlu	Hunan, China	Tree
7	CX	CX	Hubei, China	Tree	20	YZ21C	Zishou	Zhejiang, China	Tree
8	DHB	Dahua Bai	Zhejiang, China	Tree	21	YZ-5	Ziqiao	Zhejiang, China	Tree
9	DHZX	Dahua Zhaoxia	Zhejiang, China	Tree	22	YZH	Yanzhi Hong	Anhui, China	Tree
10	EW3	Ewei No. 3	Hubei, China	Tree	23	ZJL	Zi Jingling	Hunan, China	Tree
11	HF	Huanfen	Fujian, China	Tree	24	2017USA38	Jinlan	Zhejiang, China	Tree
12	HHQ	Honghuoqiu	United States	Tree	25	2019Z7	Meirenji	Zhejiang, China	Tree
13	HS	Hongsheng	Zhejiang, China	Tree					

4.2. Experimental Design

Seeds were treated in a 55 °C water bath for 30 min, soaked in 50 mg L^{-1} GA_3 (Yuanye Bio, Shanghai, China) for 24 h, surface-sterilized with 10% sodium hypochlorite (Sinopharm Chemical Reagent Co., Ltd., Shanghai, China) for 10 min [51], and rinsed five times with sterile water. Thirty seeds were placed in each Petri dish lined with two layers of filter paper, with three replicates [52], and incubated for 14 d at 26 °C, 2500 lx, 60% relative humidity, and a 16 h light/8 h dark photoperiod. Healthy, uniform seedlings were transplanted into 50-cell trays containing vermiculite–peat (1:1, *v*/*v*), irrigated with deionized water, and grown for 60 d. For hydroponics, roots were rinsed and seedlings were acclimated for 7 d in 10 L of half-strength Hoagland solution (pH 5.8) with continuous aeration; the solution was renewed every 3 d [53]. Seedling growth and hydroponics used the same environmental settings as germination. In a preliminary screen, four randomly selected materials were exposed to 0, 1000, 2000, 3000, 4000, 5000, 6000, or 7000 μmol L^{-1} $CdCl_2$ for 7 d, with three replicates per concentration. At 3000 μmol L^{-1}, leaves showed clear chlorosis and wilting without plant death, so this concentration was used subsequently [54]. For the main experiment, six uniform plants per material were randomly assigned to control or Cd treatment, with three independent plants per group and separate hydroponic containers for the two groups. The $CdCl_2$ concentration in the nutrient solution was raised to 1000, 2000, and 3000 μmol L^{-1} on days 1, 2, and 3, respectively, and then maintained at 3000 μmol L^{-1} for 7 d (10 d total) [55]. The solution was renewed every 3 d. Controls received no $CdCl_2$ but were renewed in the same way. At the end of treatment, leaves were collected for physiological assays, ion concentration measurements, and transcriptomic analysis. Cuttings of the Cd-tolerant material YZ21C and the Cd-sensitive material DHZX were taken from the respective mother plants, with each material propagated from a single clone. After 60 d in substrate and 7 d of hydroponic acclimation, cuttings were divided into control and Cd-treated groups and treated as described above, with three independent cuttings per group as biological replicates. At the end of treatment, leaves were collected for physiological assays, ion concentration measurements, and transcriptomic analysis.

4.3. Measurements and Experimental Procedures

Chlorophyll a, chlorophyll b, and carotenoid contents were determined by ethanol extraction [56]. SP content was measured using the Coomassie Brilliant Blue G-250 assay [57]. SOD and POD activities were determined using the NBT photoreduction and guaiacol methods, respectively, with assay kits from Suzhou Comin Biotechnology Co., Ltd. (Suzhou, China; SOD, Cat. No. SOD-2-Y; POD, Cat. No. POD-2-Y). CAT activity, MDA content, and Pro content were determined using the visible colorimetric, TBA colorimetric, and acid ninhydrin colorimetric methods, respectively, with assay kits from Suzhou Grace Biotechnology Co., Ltd. (Suzhou, China; CAT, Cat. No. G0106F; MDA, Cat. No. G0109F; Pro, Cat. No. G0111F). FW denotes fresh weight. The contents of chlorophyll a, chlorophyll b, carotenoids, and SP are expressed as mg g^{-1} FW. SOD and POD activities are expressed as U g^{-1} FW, CAT activity as μmol min^{-1} g^{-1} FW, MDA content as nmol g^{-1} FW, and Pro content as μg g^{-1} FW.

4.4. Determination of Cd Concentration and Calculation of BAF and TF

Cd concentrations in roots, stems, and leaves were determined in accordance with GB 5009.268–2025 [58]. Briefly, dried, powdered samples (0.2000 ± 0.0001 g) were mixed with 5 mL of guaranteed-reagent-grade nitric acid and allowed to stand overnight. The samples were then digested using a preset program in a microwave digestion system (Aurora 6, Shanghai Yiyao, Shanghai, China). The resulting digests were diluted to a final volume of 20 mL, and Cd concentrations were determined by inductively coupled plasma mass

spectrometry (ICP–MS; NexION 2000, PerkinElmer, Waltham, MA, USA) using external calibration. Reagent blanks were used for background correction. Three biological replicates were included for each treatment. Bioconcentration factors (BAFs) for roots, stems, and leaves, as well as translocation factors (TFs) for stem-to-root and leaf-to-root Cd transport, were calculated based on the Cd concentrations in the respective tissues.

$$\mathrm{BAF}_i = \frac{C_i}{C_{\mathrm{solution}}}, \mathrm{TF}_{\mathrm{stem/root}} = \frac{C_{\mathrm{stem}}}{C_{\mathrm{root}}}, \mathrm{TF}_{\mathrm{leaf/root}} = \frac{C_{\mathrm{leaf}}}{C_{\mathrm{root}}}$$

where C_i is the Cd concentration in roots, stems, or leaves ($\mathrm{mg \cdot kg^{-1}}$ DW), and C_{solution} is the Cd concentration in the nutrient solution ($\mathrm{mg \cdot L^{-1}}$). At a $CdCl_2$ concentration of 3000 $\mu\mathrm{mol \cdot L^{-1}}$, the corresponding Cd^{2+} concentration was 337.23 $\mathrm{mg \cdot L^{-1}}$. Accordingly, BAF is expressed in $\mathrm{L \cdot kg^{-1}}$, whereas TF is dimensionless.

4.5. Transcriptome Sequencing and Analysis

Leaves of the Cd-tolerant genotype YZ21C and Cd-sensitive genotype DHZX were collected from control (CK) and Cd-treated groups (three biological replicates per group). Total RNA was extracted, and samples meeting the quality criteria (concentration ≥ 50 ng $\mu\mathrm{L^{-1}}$, $A_{260}/A_{280} = 1.8$–2.0, A-grade) were subjected to paired-end 150-bp (PE150) sequencing on a GenoLab M platform (Zhenmai, Shenzhen, China).After adapter trimming and quality filtering, clean reads were mapped to the *Lagerstroemia indica* reference genome (329.14 Mb, 24 pseudochromosomes; NCBI BioProject: PRJNA1058153) using STAR (v2.7.11). Gene-level counts were obtained using RSEM (v1.3.0). The count data were normalized using the trimmed mean of M-values (TMM) method in edgeR (dispersion fixed at 0.01). DEGs were identified by comparing Cd-treated and CK groups for each genotype, using thresholds of FDR < 0.05 and $|\log_2 \mathrm{FC}| \geq 1$. These DEGs were further classified into shared DEGs, YZ21C comparison-specific DEGs, and DHZX comparison-specific DEGs. To descriptively assess the expression directionality of shared DEGs, a scatter plot was generated based on their $\log_2$FC values in both genotypes. KEGG enrichment analysis was performed on the OmicShare platform using plant KO pathways as the background, with p values calculated via the hypergeometric test and adjusted using the Benjamini–Hochberg method (adjusted $p < 0.05$).For validation, ten DEGs were randomly selected for quantitative real-time PCR (qRT-PCR). Primers were designed using Primer-BLAST (Primer3 version 2.5.0) (Table S10) [59], with *LiEF-1α* as the internal reference gene. cDNA was synthesized from 1 µg of total RNA. Each 20-µL qRT-PCR reaction contained 10 µL of 2× SYBR Green Master Mix, 0.4 µL of each primer, and 2 µL of cDNA. Each sample was run with three technical replicates, and relative expression levels were calculated using the $2^{-\Delta\Delta Ct}$ method.

4.6. Data Processing

Data were organized using Microsoft Excel. Statistical analyses were performed using SPSS Statistics v24.0. Figures were generated using Origin 2024 and GraphPad Prism 10, and figure panels were assembled using Adobe Illustrator 2025. TI was calculated as the ratio of the measured value in the Cd-treated group to that in the control group [60]. Because MDA is a negative indicator, its TI was calculated as the ratio of the control value to the Cd-treated value. Thus, a higher TI for MDA indicates less membrane damage [61]. For all other indicators, TI was calculated as the ratio of the Cd-treated value to the control value. The Cd tolerance of the 25 crape myrtle materials was comprehensively evaluated using PCA in combination with the membership function method. PCA based on the TI values of 11 indicators retained six principal components, explaining 84% of the total variance. The membership function values, weights, and the comprehensive Cd-tolerance value (D) were calculated. A higher D value indicates greater overall Cd tolerance. Using TI values, the 25 crape myrtle materials were grouped into four Cd-tolerance categories by

Euclidean distance (cutoff = 0.3): highly Cd-tolerant, Cd-tolerant, moderately Cd-tolerant, and Cd-sensitive.

5. Conclusions

By evaluating growth and physiological traits in 25 crape myrtle accessions under Cd stress using principal component analysis and the membership function method, we identified YZ21C as Cd-tolerant and DHZX as Cd-sensitive. Subsequent hydroponic experiments with cuttings showed that YZ21C exhibited a "high accumulation, low damage" pattern: despite having higher Cd concentrations in all organs than DHZX, its photosynthetic pigment and MDA contents remained relatively stable, suggesting greater tissue-level tolerance. Transcriptomic analysis further showed that comparison-specific differentially expressed genes (DEGs) in YZ21C were enriched in pathways associated with MAPK signaling, glutathione metabolism, and flavonoid biosynthesis, whereas those in DHZX were mainly enriched in fatty acid degradation and the tricarboxylic acid cycle. The expression patterns of selected genes were validated by qRT-PCR. The Cd-tolerant germplasm identified in this study may provide valuable resources for greening applications in Cd-contaminated areas, while the candidate pathways offer leads for molecular breeding and further studies of Cd tolerance in crape myrtle.

Supplementary Materials: The following supporting information can be downloaded at https://www.mdpi.com/article/10.3390/plants15223572/s1: Table S1: Cadmium tolerance coefficients (tolerance index, TI) of 25 Lagerstroemia indica materials; Table S2: Membership function values for comprehensive evaluation of Cd tolerance in 25 Lagerstroemia indica materials; Table S3: Principal component analysis (PCA) results of physiological indices under Cd stress; Table S4: Quality control of transcriptome sequencing data for YZ21C and DHZX materials; Table S5: Differentially expressed genes (DEGs) in YZ21C; Table S6: Differentially expressed genes (DEGs) in DHZX; Table S7: Expression changes in shared differentially expressed genes in YZ21C and DHZX under Cd treatment; Table S8: KEGG pathway enrichment results for common, Y-comparison-specific, and D-comparison-specific DEGs; Table S9: qRT-PCR results (Target_Ct) and transcriptome expression (FPKM) of the 10 selected genes; Table S10: Primer sequences used for qRT-PCR validation; Table S11. Detailed sample-to-library mapping for the RNA-seq data deposited in the GSA database (CRA051821); Figure S1: Transcriptome correlation heatmap; Figure S2: Scatter plot of shared DEGs.

Author Contributions: Conceptualization, L.N., Z.C. and M.W.; plant sample preparation, M.W., J.W., Z.Q. and G.M. and Q.H.; investigation and formal analysis, M.W. and L.N. All authors have read and agreed to the published version of the manuscript.

Funding: This research was funded by the Project of Zhejiang Provincial Research Institutes, grant number 2026F1065-1-3.

Data Availability Statement: The raw sequence data reported in this paper have been deposited in the Genome Sequence Archive in National Data Center, China National Center for Bioinformation/Beijing Institute of Genomics, Chinese Academy of Sciences (GSA: CRA051821), and are publicly accessible at https://ngdc.cncb.ac.cn/gsa (accessed on 7 November 2026).

Conflicts of Interest: Qing He was employed by Hangzhou Yuanjian Landscape Architecture Co., Ltd. The remaining authors declare that the research was conducted in the absence of any commercial or financial relationships that could be construed as a potential conflict of interest.

References

1. Shetty, B.R.; Jagadeesha, P.B.; Salmataj, S.A. Heavy metal contamination and its impact on the food chain: Exposure, bioaccumulation, and risk assessment. *CyTA J. Food* **2025**, *23*, 2438726. [CrossRef]
2. Hou, D.; Jia, X.; Wang, L.; McGrath, S.P.; Zhu, Y.G.; Hu, Q.; Zhao, F.J.; Bank, M.S.; O'Connor, D.; Nriagu, J. Global soil pollution by toxic metals threatens agriculture and human health. *Science* **2025**, *388*, 316–321. [CrossRef]

3. Ministry of Environmental Protection of the People's Republic of China; Ministry of Land and Resources of the People's Republic of China. Report on the National General Survey of Soil Contamination. Available online: https://www.mee.gov.cn/gkml/sthjbgw/qt/201404/t20140417_270670.htm (accessed on 28 September 2026).
4. Deepika; Haritash, A.K. Phytoremediation potential of ornamental plants for heavy metal removal from contaminated soil: A critical review. *Hortic. Environ. Biotechnol.* **2023**, *64*, 709–734. [CrossRef]
5. Cozma, P.; Roșca, M.; Minuț, M.; Gavrilescu, M. Phytoremediation: A sustainable and promising bio-based approach to heavy metal pollution management. *Sci. Total Environ.* **2025**, *1001*, 180458. [CrossRef]
6. Chen, G.X.; Zhou, H.M.; Chen, H.J.; Chen, S.S.; Feng, J.; Liu, X.T.; Deng, L.; Deng, Y.M. Technical analysis and prospects of using ornamental plants to remediate urban lead-contaminated soils. *J. Plant Resour. Environ.* **2025**, *34*, 82–93. (In Chinese) [CrossRef]
7. Liu, Z.Y.; Liu, X.Y.; Liu, S.D.; Xia, X.H.; Zhang, L.X. Heavy metal damage to ornamental horticultural and landscape plants and their responses. *Mod. Hortic.* **2025**, *48*, 18–22. (In Chinese) [CrossRef]
8. Rao, M.J.; Duan, M.; Zhou, C.; Jiao, J.; Cheng, P.; Yang, L.; Wei, W.; Shen, Q.; Ji, P.; Yang, Y.; et al. Antioxidant defense system in plants: Reactive oxygen species production, signaling, and scavenging during abiotic stress-induced oxidative damage. *Horticulturae* **2025**, *11*, 477. [CrossRef]
9. Cuypers, A.; Plusquin, M.; Remans, T.; Jozefczak, M.; Keunen, E.; Gielen, H.; Opdenakker, K.; Nair, A.R.; Munters, E.; Artois, T.J.; et al. Cadmium stress: An oxidative challenge. *BioMetals* **2010**, *23*, 927–940. [CrossRef]
10. Fan, L.; Zhou, Q.; Yang, H.; Ling, X.; Fan, W.; Tang, L. Effects of salt stress on the physiology and biochemistry of six poplar germplasms and evaluation of their salt tolerance. *Forests* **2025**, *16*, 1733. [CrossRef]
11. Cheng, Q.; Wang, C.; Zhao, B. Comprehensive evaluation of the response of 15 Hydrangea cultivars (species) to cadmium stress. *J. Northwest A F Univ. (Nat. Sci. Ed.)* **2025**, *53*, 188–198. (In Chinese) [CrossRef]
12. Huang, S.Q.; Liu, S.; Sun, R.; Li, R.G. Comprehensive evaluation of Bougainvillea germplasm resources based on principal component analysis and membership function method. *J. South. Agric.* **2026**, *57*, 1797–1808. (In Chinese) [CrossRef]
13. Zhang, H.; Chen, J.; Wang, W.; Li, Q.; Zhang, W.; Li, B.; Zhang, X.; Hu, J.; Wang, Z.; Liu, Y.; et al. Integrated transcriptomic and metabolomic analysis reveals the molecular mechanisms of cadmium stress response in rapeseed (*Brassica napus* L.): Insights into glutathione and sulfur metabolism pathways. *Ind. Crops Prod.* **2025**, *237*, 122187. [CrossRef]
14. Zheng, J.; Wang, X.; Huang, R.; Xian, P.; Cui, J.; Amo, A.; Chen, L.; Han, Y.; Hou, S.; Yang, Y. Integration of comparative cytology, ionome, transcriptome and metabolome provide a basic framework for the response of foxtail millet to Cd stress. *J. Hazard. Mater.* **2025**, *489*, 137684. [CrossRef]
15. Dong, Q.; Wu, Y.; Li, B.; Chen, X.; Peng, L.; Sahito, Z.A.; Li, H.; Chen, Y.; Tao, Q.; Xu, Q.; et al. Multiple insights into lignin-mediated cadmium detoxification in rice (*Oryza sativa*). *J. Hazard. Mater.* **2023**, *458*, 131931. [CrossRef]
16. Wu, F.; Fan, J.; Ye, X.; Yang, L.; Hu, R.; Ma, J.; Ma, S.; Li, D.; Zhou, J.; Nie, G.; et al. Unraveling cadmium toxicity in *Trifolium repens* L. seedling: Insight into regulatory mechanisms using comparative transcriptomics combined with physiological analyses. *Int. J. Mol. Sci.* **2022**, *23*, 4612. [CrossRef]
17. Sun, L.; Yan, T.; Wang, T.; Zhu, J.; Shu, X.; Wang, Z.; Zhuang, W. Integrated physiological, transcriptomic and metabolomic analysis revealed key genes related to cadmium-stress tolerance in poplar. *J. Hazard. Mater.* **2025**, *500*, 140557. [CrossRef]
18. Zhang, H.; Zhang, X.; Liu, H.; Zhang, Y.; Fang, J.; Li, T.; Yang, N.; Da, L. Integrated physiological, metabolomic, and transcriptomic analyses reveal the differential molecular mechanisms underlying cadmium stress responses in two *Codonopsis pilosula* cultivars. *Ind. Crops Prod.* **2026**, *239*, 122428. [CrossRef]
19. Zhao, Q.S.; Cheng, T.T.; Sun, Z.K.; Yan, Y.; Han, X.; Du, H. Research progress on germplasm resources and breeding of *Lagerstroemia indica*. *Northwest Hortic.* **2026**, *6*, 8–11. (In Chinese)
20. Xu, J.Y.; Jing, D.Z.; Zhou, C.H. Application of *Lagerstroemia indica* in landscape greening. *Agric. Dev. Equip.* **2020**, *9*, 221–222. (In Chinese)
21. Wang, S.H.; Luo, Y.; Ji, H.L.; Liu, Y.; Li, B.G.; Song, X.M. Current status and future perspectives of *Lagerstroemia* breeding in China. *Acta Agric. Jiangxi* **2025**, *37*, 32–38. (In Chinese) [CrossRef]
22. Zhang, L.J.; Li, X.M.; Feng, S.C. Research progress on germplasm resources and application of *Lagerstroemia indica*. *Guangdong Agric. Sci.* **2024**, *51*, 81–91. (In Chinese) [CrossRef]
23. Liang, C. Screening of suitable tree species for ecological restoration of derelict copper mining lands. *Anhui Agric. Sci. Bull.* **2025**, *31*, 40–43. (In Chinese) [CrossRef]
24. Li, J.; Li, Y.; Zi, D.; Zhai, F.; Deng, S.; Zhang, Y. Comparative tolerance and phytoremediation potential of four *Lagerstroemia indica* cultivars under cadmium stress. *Sci. Rep.* **2025**, *16*, 2014. [CrossRef]
25. Adeosun, A.; Price, A.; Norton, G. Cadmium tolerance and accumulation in wild rice species. *Rice Sci.* **2023**, *30*, 181–185. [CrossRef]
26. Touati, M.; Bottega, S.; Castiglione, M.R.; Sorce, C.; Béjaoui, Z.; Spanò, C. Modulation of the defence responses against Cd in willow species through a multifaceted analysis. *Plant Physiol. Biochem.* **2019**, *142*, 125–136. [CrossRef]

27. Zhang, X.Q.; Li, Z.Z.; Chen, S.B.; Wang, X.H.; Duan, G.L. Differences in sensitivity of shrub seedlings to cadmium toxicity. *J. Agric. Sci. Technol.* **2022**, *24*, 173–184. (In Chinese) [CrossRef]
28. Wu, Y.; Yao, Y.; Gong, B.; Wang, Y.; Dong, X.; Zeng, C.; Liu, Z. Mechanism of cadmium tolerance in *Brassica juncea*: An insight from comparative physiology and transcriptomics of two cultivars. *Planta* **2026**, *263*, 93. [CrossRef]
29. Song, J.; Sun, Z.; Saud, S.; Fahad, S.; Nawaz, T. Exploring the deleterious effects of heavy metal cadmium on antioxidant defense and photosynthetic pathways in higher plants. *Plant Stress* **2025**, *15*, 100716. [CrossRef]
30. Jia, L.; Yu, G.; Zhao, Z.; Lü, L. Effects of cadmium (Cd) on photosynthetic characteristics and chlorophyll fluorescence parameters in the ornamental plant *Salvia splendens* Ker-Gawl. *Physiol. Mol. Biol. Plants* **2025**, *31*, 507–519. [CrossRef]
31. Saoudi, W.; Boubakri, H.; Taamalli, W.; Debez, A.; Abdelly, C. Differential reduction in cadmium accumulation in barley under cadmium-salt co-exposure involves specific HMA genes and antioxidative responses. *Environ. Exp. Bot.* **2024**, *225*, 105852. [CrossRef]
32. Gill, S.S.; Tuteja, N. Reactive oxygen species and antioxidant machinery in abiotic stress tolerance in crop plants. *Plant Physiol. Biochem.* **2010**, *48*, 909–930. [CrossRef]
33. Mushtaq, G.; Agrawal, S.; Kushwah, A.; Kumar, A.; Lone, R. Cadmium toxicity in plants and its remediation management: A review. *Plant Stress* **2025**, *16*, 100894. [CrossRef]
34. Sun, Y.; Hu, R.; Yang, J.; Li, C.; Xue, J.; Zhang, Z.; Li, R.; Jia, X. Transcriptome and metabolome atlas reveals pivotal roles of glutathione and nicotianamine metabolism in Cd stress resistance in oat. *Plant Physiol. Biochem.* **2026**, *232*, 111080. [CrossRef]
35. Barman, F.; Majumdar, S.; Arzoo, S.H.; Kundu, R. Genotypic variation among 20 rice cultivars/landraces in response to cadmium stress grown locally in West Bengal, India. *Plant Physiol. Biochem.* **2020**, *148*, 193–206. [CrossRef]
36. Sheng, S.S.; Liu, R.P.; Wang, X.Y.; Yuan, J. Physiological and metabolomic analysis of *Plantago asiatica* L. in response to cadmium stress. *Plant Sci. J.* **2023**, *41*, 234–244. (In Chinese) [CrossRef]
37. Gong, J.; Wang, C.; Wang, J.; He, J.; Li, J.; Zhang, X.; Wang, Y.; Chen, L.; Liu, H.; Zhao, X.; et al. Integrative study of transcriptome and microbiome to reveal the response of *Rhododendron decorum* to cadmium stress. *Ecotoxicol. Environ. Saf.* **2024**, *280*, 116536. [CrossRef]
38. Zhang, T.; Pang, W.; Yan, T.; Zhang, P.; He, J.; Rensing, C.; Yang, W.; Lian, C. Metal-non-tolerant ecotypes of ectomycorrhizal fungi can protect plants from cadmium pollution. *Front. Plant Sci.* **2023**, *14*, 1301791. [CrossRef]
39. Zhao, X.; Sun, J.; Han, J.; Wang, Y.; Zhang, L.; Li, W.; Chen, B.; Liu, Y. Transcriptome and metabolome analyses reveal the molecular mechanisms of *Rhododendron pulchrum* under cadmium stress. *Ecotoxicol. Environ. Saf.* **2026**, *325*, 120936. [CrossRef]
40. Liu, M.; Wu, S.; Song, Y.; Shi, M.; Yi, L. Physiological and transcriptome analysis of sex-specific responses to cadmium stress in poplars. *Ecotoxicol. Environ. Saf.* **2025**, *289*, 117675. [CrossRef]
41. Zhang, Z.; Zhong, L.; Xiao, W.; Du, Y.; Han, G.; Yan, Z.; He, D.; Zheng, C. Transcriptomics combined with physiological analysis reveals the mechanism of cadmium uptake and tolerance in *Ligusticum chuanxiong* Hort. under cadmium treatment. *Front. Plant Sci.* **2023**, *14*, 1263981. [CrossRef]
42. Liu, H.; Jiao, Q.; Fan, L.; Jiang, Y.; Alyemeni, M.N.; Ahmad, P.; Chen, Y.; Zhu, M.; Liu, H.; Zhao, Y.; et al. Integrated physio-biochemical and transcriptomic analysis revealed mechanism underlying of Si-mediated alleviation to cadmium toxicity in wheat. *J. Hazard. Mater.* **2023**, *452*, 131366. [CrossRef]
43. Sun, Y.; Liu, X.; Li, W.; Wang, X.; Zhong, X.; Gao, Y.; Xu, H.; Hu, H.; Zhang, L.; Cheng, X.; et al. The regulatory metabolic networks of the *Brassica campestris* L. hairy roots in response to cadmium stress revealed from proteome studies combined with a transcriptome analysis. *Ecotoxicol. Environ. Saf.* **2023**, *263*, 115214. [CrossRef]
44. Wang, J.; Yang, L.; Xu, B.; Cao, R.; Charagh, S.; Hui, S.; Zhou, L.; Zhang, Y.; Chen, Y.; Sheng, Z.; et al. Chloroplast-localized transporter OsNTP1 mediates cadmium transport from root to shoot and sugar metabolism in rice. *J. Hazard. Mater.* **2025**, *484*, 136766. [CrossRef]
45. Tian, Y.S.; She, J.J.; Chen, F.; Ren, H.C.; Wang, Y.F.; Dang, F.F. AtGRF5 enhances cadmium tolerance in *Arabidopsis* by regulating the antioxidant system and JA signaling pathway. *J. Yan'an Univ. (Nat. Sci. Ed.)* **2026**, *45*, 43–50. (In Chinese) [CrossRef]
46. Zhang, M.; Yu, X.; Teng, Z.; Wei, C.; Teng, K.; Fan, Z.; Xie, Y.; Cao, X.; Li, M.; Ma, S.; et al. Multi-omics analysis reveals the dynamic adaptive mechanisms of rice seedlings in response to cadmium stress. *Environ. Exp. Bot.* **2026**, *248*, 106404. [CrossRef]
47. Boro, P.; Chattopadhyay, S. Crosstalk between MAPKs and GSH under stress: A critical review. *J. Biosci.* **2022**, *47*, 71. [CrossRef]
48. Bellini, E.; Bandoni, E.; Giardini, S.; Sorce, C.; Spanò, C.; Bottega, S.; Fontanini, D.; Kola, A.; Valensin, D.; Bertolini, A.; et al. Glutathione and phytochelatins jointly allow intracellular and extracellular detoxification of cadmium in the liverwort *Marchantia polymorpha*. *Environ. Exp. Bot.* **2023**, *209*, 105303. [CrossRef]
49. Zhou, J.; Ji, P.; Liu, G.; Wang, S.; Liu, L.; Liu, C.; Sun, G.; Xue, S.; Du, Y.; Li, H. The SeABI5 transcription factor couples ABA signaling with flavonoid antioxidant production to confer cadmium tolerance in *Salicornia europaea*. *J. Hazard. Mater.* **2026**, *516*, 143448. [CrossRef]
50. Wu, M.; Xu, Q.; Tang, T.; Li, X.; Pan, Y. Integrative physiological, transcriptomic, and metabolomic analysis of *Abelmoschus manihot* in response to Cd toxicity. *Front. Plant Sci.* **2024**, *15*, 1396124. [CrossRef]

51. Ma, D.Y.; Yan, N.; Xu, J.; Du, J.M.; Zhu, C.Y. Study on fruit morphological characteristics and seed germination of *Lagerstroemia indica*. *Mod. Agric. Sci. Technol.* **2024**, *13*, 64–68. (In Chinese) [CrossRef]
52. Gu, C.H.; Zhang, Q.X. Study on seed germination characteristics of *Lagerstroemia indica*. *North. Hortic.* **2007**, *9*, 141–142. (In Chinese)
53. Feng, Q.; Tai, P.D.; Fu, S.S.; Wang, X.J.; Zhang, Y. The possible mechanisms of cadmium accumulation in *Tagetes erecta* L. under macronutrient deficiency. *Appl. Mech. Mater.* **2012**, *178–181*, 1060–1064. [CrossRef]
54. Wei, Y.; Liao, L.Q.; Liu, N.R.; Chen, F.F.; Zhang, L.M.; Zhang, H.; Long, W.; Liu, H.Q.; Pang, B.; Zhu, H.Q.; et al. Comprehensive evaluation and index screening of cadmium tolerance difference in seedlings of different sweet potato varieties. *Jiangsu Agric. Sci.* **2025**, *53*, 38–45. (In Chinese) [CrossRef]
55. Yang, W.; Wu, F.; Ding, Z.; Zhang, X.; Zhao, F.; Wang, Y.; Yang, X. Cadmium Accumulation and Tolerance in Seven Ornamental Willow Genotypes. *Bull. Environ. Contam. Toxicol.* **2018**, *101*, 644–650. [CrossRef]
56. Lichtenthaler, H.K. Chlorophylls and carotenoids: Pigments of photosynthetic biomembranes. In *Methods in Enzymology*; Packer, L., Douce, R., Eds.; Academic Press: New York, NY, USA, 1987; Volume 148, pp. 350–382. [CrossRef]
57. Bradford, M.M. A rapid and sensitive method for the quantitation of microgram quantities of protein utilizing the principle of protein-dye binding. *Anal. Biochem.* **1976**, *72*, 248–254. [CrossRef]
58. *GB 5009.268—2025*; National Food Safety Standard—Determination of Multi-elements in Foods. Standards Press of China: Beijing, China, 2025.
59. Ye, J.; Coulouris, G.; Zaretskaya, I.; Cutcutache, I.; Rozen, S.; Madden, T.L. Primer-BLAST: A tool to design target-specific primers for polymerase chain reaction. *BMC Bioinform.* **2012**, *13*, 134. [CrossRef]
60. Iqbal, M.Z.; Rahmati, K.; Iqbal, M.Z. Tolerance of *Albizia lebbeck* to Cu and Fe application. *Ekologia (CSFR)* **1992**, *11*, 427–430.
61. Qiu, Y.; Wei, S.; Zhan, J.; Robinson, B.H.; Skuza, L.; Xue, J.; Dai, H.; Zhan, L.; Tang, Z. Physio-biochemical indexes as indicators of cadmium tolerance in *Brassica napus* L. cultivars. *Agriculture* **2025**, *15*, 132. [CrossRef]

Disclaimer/Publisher's Note: The statements, opinions and data contained in all publications are solely those of the individual author(s) and contributor(s) and not of MDPI and/or the editor(s). MDPI and/or the editor(s) disclaim responsibility for any injury to people or property resulting from any ideas, methods, instructions or products referred to in the content.